

# Isoprene and Monoterpene Emission Rate Variability: Model Evaluations and Sensitivity Analyses

ALEX B. GUENTHER, PATRICK R. ZIMMERMAN, AND PETER C. HARLEY

*Atmospheric Chemistry Division, National Center for Atmospheric Research, Boulder, Colorado*

RUSSELL K. MONSON

*Department of EPO Biology, University of Colorado, Boulder*

RAY FALL

*Department of Chemistry and Biochemistry and Cooperative Institute for Research in Environmental Sciences,  
University of Colorado, Boulder*

The emission of isoprene and monoterpenes from plants is influenced by light and leaf temperature, which account for almost all short-term variations (minutes to days) and a large part of spatial and long-term variations. The temperature dependence of monoterpene emission varies among monoterpenes, plant species, and other factors, but a simple exponential relationship between emission rate ( $E$ ) and leaf temperature ( $T$ ),  $E = E_s [\exp (\beta(T - T_s))]$ , provides a good approximation. A review of reported measurements suggests a best estimate of  $\beta = 0.09 \text{ K}^{-1}$  for all plants and monoterpenes. Isoprene emissions increase with photosynthetically active radiation up to a saturation point at  $700\text{--}900 \mu\text{mol m}^{-2} \text{ s}^{-1}$ . An exponential increase in isoprene emission is observed at leaf temperatures of less than  $30^\circ\text{C}$ . Emissions continue to increase with higher temperatures until a maximum emission rate is reached at about  $40^\circ\text{C}$ , after which emissions rapidly decline. This temperature dependence can be described by an enzyme activation equation that includes denaturation at high temperature. Algorithms developed to simulate these light and temperature responses perform well for a variety of plant species under laboratory and field conditions. Evaluations with field measurements indicate that these algorithms perform significantly better than earlier models which have previously been used to simulate isoprene emission rate variation. These algorithms account for about 90% of observed diurnal variability and can predict diurnal variations in hourly averaged isoprene emissions to within 35%.

## 1. INTRODUCTION

Isoprene and monoterpenes are volatile hydrocarbon compounds that are produced by vegetation and emitted into the atmosphere in significant quantities. Emissions of biogenic hydrocarbons are estimated to equal or exceed anthropogenic emissions even in industrialized nations such as the United States [Lamb *et al.*, 1987]. Biogenic and anthropogenic hydrocarbons can influence the chemical composition of the atmosphere by controlling the oxidation capacity of the troposphere [Chameides *et al.*, 1988]. In regions with sufficient levels of oxides of nitrogen and sunlight, this influence can include photochemical production of ozone and peroxides [Liu *et al.*, 1987]. Highly reactive biogenic hydrocarbons play a major role in photochemical oxidant production even when they are present in the atmosphere at concentrations that are much lower than those of anthropogenic hydrocarbons [Chameides *et al.*, 1992].

Numerical tropospheric photochemistry models typically use time steps of less than 1 min [e.g., Roselle *et al.*, 1991]. Diurnally varying boundary conditions must be specified for sources such as biogenic hydrocarbon emissions, which can vary several orders of magnitude in a 24-hour period. Diurnal variations in biogenic hydrocarbon emissions are controlled by changes in light and/or temperature. Light and

temperature also strongly influence seasonal and spatial variations [see Lamb *et al.*, 1987].

In this paper we describe and evaluate models which simulate short-term variations in isoprene (section 2) and monoterpene (section 3) emissions from plants. In section 2.1 we describe two isoprene emission rate data bases which are referred to in this paper. A laboratory measurement data base was used in the development of an isoprene emission model, and a field measurement data base was used to evaluate the new model and eight previously published models. Section 2.2 provides a detailed description of the new isoprene emission model and brief descriptions of the other eight models. The performance of each model is evaluated in section 2.3, and the results of sensitivity analyses are included in section 2.4. A simple model for monoterpene emissions is described and evaluated in section 3.1, and model sensitivity analyses are discussed in section 3.2. These results are summarized in section 4, and specific recommendations for biogenic isoprene and monoterpene emission rate modeling are provided.

## 2. ISOPRENE EMISSIONS

### 2.1. Isoprene Emission Rate Measurements

A data base of isoprene emission rate measurements from individual leaves of sweet gum (*Liquidambar styraciflua*) and aspen (*Populus tremuloides*) trees at nine light intensities and 12 leaf temperatures was made for this study. These

Copyright 1993 by the American Geophysical Union.

Paper number 93JD00527.  
0148-0227/93/93JD-00527\$05.00

TABLE 1. Isoprene Emission Rate Models

Model	Description	Driving Variables*	Reference
G91	Emissions vary with temperature and light. Model coefficients were determined by best fit to laboratory emission rate measurements of eucalyptus trees.	<i>T, L</i>	<i>Guenther et al.</i> [1991]
G93	Emissions vary with temperature and light. Model coefficients were determined by best fit to laboratory emission rate measurements of four plant species.	<i>T, L</i>	Equations (1)–(3)
T400	Emissions are zero at night and increase sigmoidally with temperature during the day. Coefficients were determined by best fit to laboratory emission rate measurements of live oak trees under PAR flux of 400 $\mu\text{mol m}^{-2} \text{s}^{-1}$ .	<i>T, H</i>	<i>Tingey et al.</i> [1981]
T800	Emissions are zero at night and increase sigmoidally with temperature during the day. Coefficients were determined by best fit to laboratory emission rate measurements of live oak trees under PAR flux of 800 $\mu\text{mol m}^{-2} \text{s}^{-1}$ .	<i>T, H</i>	<i>Tingey et al.</i> [1981]
BEIS	Influences of temperature and light are estimated by interpolating between estimates from four Tingey curves, which include models T400 and T800 and curves for 100 and 200 $\mu\text{mol m}^{-2} \text{s}^{-1}$ . Emissions are zero at night.	<i>T, L</i>	<i>Pierce and Waldruff</i> [1991]
EES	Emissions vary with temperature and light. Model coefficients were determined by best fit to laboratory emission rate measurements of Engelmann spruce trees.	<i>T, L</i>	<i>Evans et al.</i> [1985]
ESS	Emissions vary with temperature and light. Model coefficients were determined by best fit to laboratory emission rate measurements of Sitka spruce trees.	<i>T, L</i>	<i>Evans et al.</i> [1985]
L87	Emissions are zero at night and increase exponentially with temperature during the day. Coefficient was determined by best fit to emission rate data from a variety of plant species, field sites, and seasons.	<i>T, H</i>	<i>Lamb et al.</i> [1987]
HR	Emissions are zero at night and constant at midday and increase (decrease) linearly with time in the morning (afternoon).	<i>H</i>	<i>Chameides et al.</i> [1988]

\**T*, temperature; *L*, PAR; *H*, hour of day.

data were combined with similar measurements of isoprene emission from eucalyptus trees (*Eucalyptus globulus*) and velvet beans (*Mucuna pruriens*), which have been described elsewhere [Guenther et al., 1991; Monson et al., 1992]. The plants were grown in a greenhouse with supplemental lighting and were fertilized weekly. Isoprene emission rates were measured with a real-time, fast-response chemiluminescence analyzer [Hills and Zimmerman, 1990] and a gas exchange and environmental control system [Monson et al., 1991]. The chemiluminescence analyzer was calibrated with a gas mixture referenced to National Institute of Standards and Technology (NIST) Standard Reference Material (SRM 1660a; 1 ppm propane in  $\text{N}_2$ ). Emission rates from each leaf were measured at temperatures between 18 and 45°C (with 3°C increments) or at seven to nine levels of photosynthetically active radiation (PAR).

Isoprene emission rates were measured during June and July 1990 at a field site in eastern Alabama. Details of this study are described by A. Guenther et al. (Biogenic hydrocarbon fluxes from forests in the southeastern United States, submitted to *Journal of Geophysical Research*, 1993, hereinafter referred to as Guenther et al., submitted manuscript, 1993). A dynamic (flow-through) enclosure technique was used to measure isoprene emissions from individual leaves or branches. Diurnal variations in isoprene emission rates from sweet gum and three species of oak (*Quercus* spp.) were measured at intervals of 30 minutes to 2 hours for periods of up to 18 hours. Six different trees were sampled for a total of 94 measurements. Leaf temperature, enclosure temperature, relative humidity, PAR, and general sampling conditions were recorded for each measurement. Photosynthesis, transpiration, and stomatal conductance measured with a LICOR 6200 system indicated that the physiological behavior of these trees was within normal limits.

## 2.2. Isoprene Model Descriptions

Table 1 contains brief descriptions of nine models which can be used to predict the effects of environmental variables on isoprene emission rates. These models include approaches developed by Guenther and coworkers (G91, G93), Tingey and coworkers (T400, T800, BEIS), Evans and coworkers (EES, ESS), Lamb and coworkers (L87), and Chameides and coworkers (HR). Each of these models except G93 has been described previously; G93 is described below.

A variety of factors influence isoprene emission rates. Although the mechanisms controlling isoprene emission are not well known, recent studies have correlated both long-term and short-term variations in isoprene emission with isoprene synthase activity [Kuzma and Fall, 1993; Monson et al., 1992]. Normal variations in humidity,  $\text{CO}_2$  concentration, and stomatal conductance play a minor role in controlling short-term variations in isoprene emissions [e.g., Guenther et al., 1991; Fall and Monson, 1992]. These studies suggest that PAR and leaf temperature can account for short-term variations in isoprene emissions. One model listed in Table 1 (HR) uses only time of day, which is a general indicator of both temperature and PAR, as a model input. Three models (T400, T800, and L87) use only temperature as an input and assume that emissions fall to zero at night. The other five models use both temperature and PAR as model inputs.

Model G93 estimates emissions as

$$I = I_s \cdot C_L \cdot C_T \quad (1)$$

where *I* is isoprene emission rate at a temperature *T*(K) and PAR flux *L* ( $\mu\text{mol m}^{-2} \text{s}^{-1}$ ), *I<sub>s</sub>* is isoprene emission rate at a standard temperature, *T<sub>s</sub>*(K), and a standard PAR flux (1000  $\mu\text{mol m}^{-2} \text{s}^{-1}$ ). The factor *C<sub>L</sub>* is defined by

$$C_L = \frac{\alpha c_{L1} L}{\sqrt{1 + \alpha^2 L^2}} \quad (2)$$

where  $\alpha$  ( $= 0.0027$ ) and  $c_{L1}$  ( $= 1.066$ ) are empirical coefficients which were determined by nonlinear best fit procedures using eucalyptus, sweet gum, aspen, and velvet bean emission rate measurements. Equation (2) simulates a nearly linear increase in isoprene emissions up to a saturation point and is similar to equations which have been used to model the light dependency of photosynthesis [e.g., *Smith, 1937; Harley and Tenhunen, 1991*]. The coefficient  $\alpha$  is the initial slope of the curve relating normalized isoprene emission to PAR and is analogous to quantum use efficiency (on an incident light basis). The coefficient  $c_{L1}$  is set to force  $C_L$  equal to 1 at the standard condition of  $1000 \mu\text{mol m}^{-2} \text{s}^{-1}$ . This coefficient could be varied to simulate the influence of additional factors (e.g., light intensity during growth) when quantitative descriptions of these relationships become available. Equation (2) provides a good approximation to the PAR responses observed for all four plant species studied. Estimates of  $\alpha$  range from  $0.002 \pm 0.0007$  for velvet bean to  $0.0036 \pm 0.0014$  for eucalyptus. Leaf-to-leaf differences in  $\alpha$  may be a result of leaf age, different growth conditions, maximum emission rates, or other factors. Additional measurements are needed to determine the importance of modeling these second-order effects. Model G93 simulates the temperature dependency of isoprene emission with equation (3), which has been used to simulate the temperature response of enzymatic activity [e.g., *Johnson et al., 1942; Sharpe and DeMichelle, 1977*].

$$C_T = \frac{\exp \frac{c_{T1}(T - T_S)}{RT_S T}}{1 + \exp \frac{c_{T2}(T - T_M)}{RT_S T}} \quad (3)$$

where  $R$  is a constant ( $= 8.314 \text{ J K}^{-1} \text{ mol}^{-1}$ ), and  $c_{T1}$  ( $= 95,000 \text{ J mol}^{-1}$ ),  $c_{T2}$  ( $= 230,000 \text{ J mol}^{-1}$ ), and  $T_M$  ( $= 314 \text{ K}$ ) are empirical coefficients which were estimated by nonlinear best fit procedures using eucalyptus, sweet gum, aspen, and velvet bean emission rate measurements. Two of the three model coefficients in equation (3),  $c_{T1}$  and  $c_{T2}$ , were nearly constant for all tested leaves. The best fit value of the coefficient  $T_M$  varied significantly. This coefficient influences the predicted emission behavior at high temperatures (above  $30^\circ\text{C}$ ). Similar ranges in estimates of  $T_M$  were determined for each of the plant species tested, which suggests that this variation is not species dependent. Growth conditions may play a role in determining the response of isoprene emission to high temperatures [*Monson et al., 1992*]. It is difficult to describe the behavior of isoprene emission at high temperatures because two opposing biochemical processes appear to be occurring: (1) the enzyme isoprene synthase is activated with increasing temperature, resulting in increased emissions; and (2) at high temperatures (e.g.,  $>33^\circ\text{C}$ ) the enzyme denatures, decreasing emissions [*Monson et al., 1992*]. Figure 1 shows that at temperatures above  $33^\circ\text{C}$ , an increase in temperature results in an initial increase in isoprene emission followed by a slow decline in emission. It is important that descriptions of measurements of isoprene emission at high temperature be accompanied by

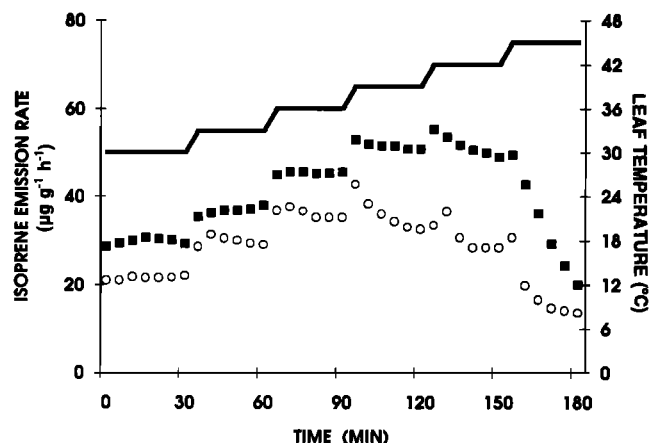


Fig. 1. Response of isoprene emission rate (open circles and solid boxes) to increases in temperature (solid line) for two different sweet gum leaves.

the amount of time that the leaf was at the temperature at which the measurement was made.

### 2.3. Isoprene Model Evaluations

In this section, we evaluate the performance of each of the isoprene emission models described in Table 1. The general behavior of the models is discussed and compared to measurements of isoprene emission rates from four plant species. The overall performance of each model is evaluated by using a field data set.

The normalized isoprene emission rates shown in Figure 2 initially increase linearly with increasing PAR but saturate at higher PAR levels. Similar behavior was observed for all four plant species. Figure 2 also demonstrates the ability of models G91, G93, BEIS, ESS, and EES to simulate this behavior. The other four models described in Table 1 do not predict emission rate variations with changes in PAR. Models G91 and G93 both provide a good fit to the observed emission rate variation with PAR. Model G93 provides a slight enhancement over model G91 by setting the normalized emission equal to 1 at a PAR of  $1000 \mu\text{mol m}^{-2} \text{s}^{-1}$ . Model BEIS consistently underpredicts normalized emission rates at a PAR of less than  $700 \mu\text{mol m}^{-2} \text{s}^{-1}$ . Model ESS consistently overpredicts normalized emission rates at low PAR values, while model EES overpredicts at very low and high PAR values and underpredicts when PAR is between 200 and  $800 \mu\text{mol m}^{-2} \text{s}^{-1}$ .

Figure 3 shows that normalized isoprene emission rates increase exponentially with leaf temperature up to temperatures of around  $35^\circ\text{C}$ . Emissions level off at this point and begin to decrease with temperatures above  $40^\circ\text{C}$ . All of the models listed in Table 1 except model HR simulate variations in emissions with changes in temperature. Only models G91, G93, ESS, and EES correctly predict the observed decrease in emissions at high temperatures. The only differences between models G91 and G93 or between models ESS and EES are the model coefficients. Model L87 correctly predicts emission rate variation at low temperatures but greatly overpredicts at high temperatures. Models T400, T800, and BEIS all underpredict normalized emissions at low temperatures. Models T800 and BEIS overpredict at

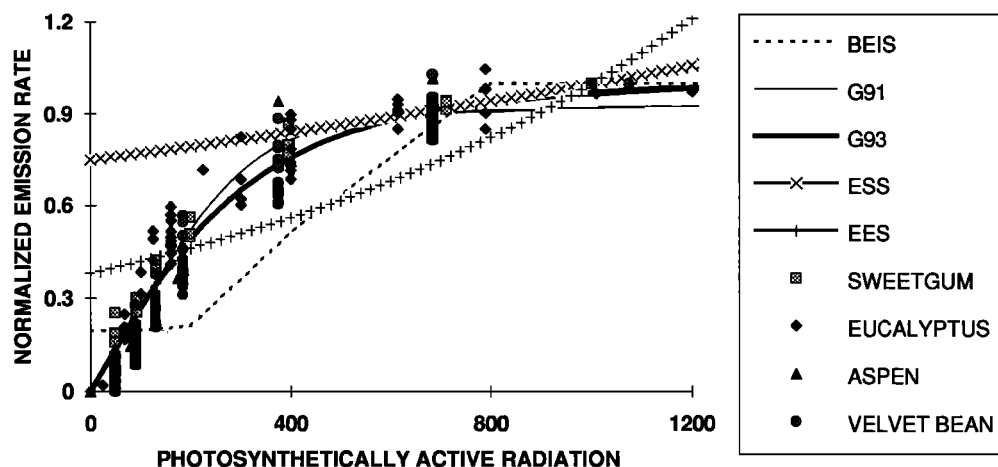


Fig. 2. Relationship between normalized isoprene emission rates and PAR values observed for sweet gum, eucalyptus, aspen, and velvet bean (symbols) and simulated by five of the isoprene emission models described in Table 1 (lines).

high temperatures, while model T400 underpredicts at high temperatures.

The field measurements of isoprene emissions described in section 2.1 were used to evaluate each isoprene emission model. The results of this evaluation are summarized in Table 2. To evaluate only the ability to predict diurnal emission rate variations, observed emission rates were normalized by the estimated emission rate at the standard condition of 30°C and 1000  $\mu\text{mol m}^{-2} \text{s}^{-1}$ . Emission rates at this standard condition were estimated by using each model to relate emissions under observed conditions to expected emissions under standard conditions. Examples of these standardized rates for a red oak leaf are given in Table 2. The wide variation in the standardized rates (34 to 71  $\mu\text{g of C g}^{-1} \text{h}^{-1}$ ) estimated by using the various models demonstrates the

importance of estimating standardized rates with a model that can accurately simulate emission rate variations.

The correlation coefficients listed in Table 2 show that 86 to 89% of the total variation in diurnal isoprene emission rates can be accounted for by models G91 and G93. Models T400, T800, BEIS, L87, and ESS account for 77 to 81% of diurnal variations, while models EES and HR account for only 61 and 33%, respectively. Percent differences between observed and predicted daily and hourly emission rates are also shown in Table 2. The hourly emission rates predicted by models G93 and G91 were within 21 to 53% of observed emissions. The mean percent differences were 36% (model G93) and 37% (model G91). Percent differences in predicted and observed hourly emissions ranged from 25 to 78% (mean = 43 to 48%) for the other seven models. The percent

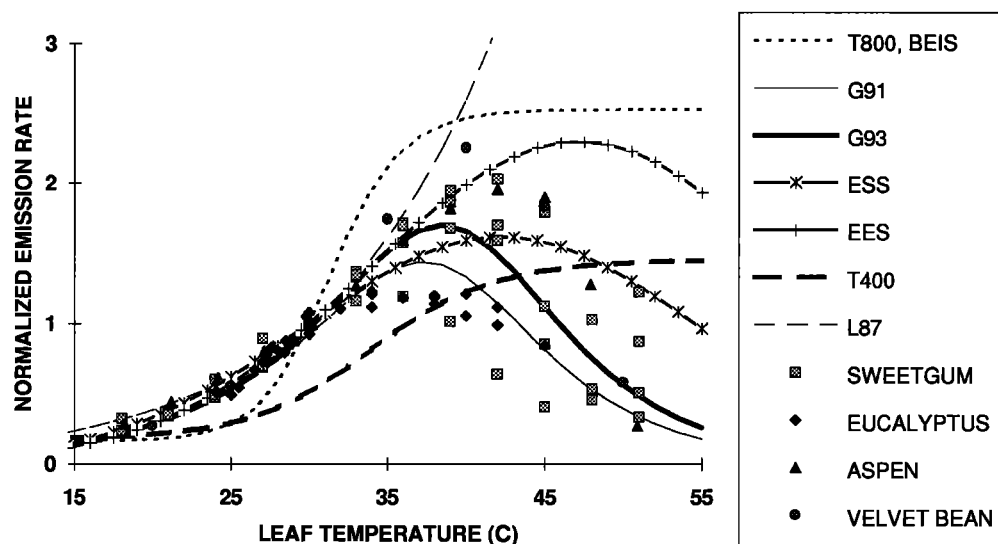


Fig. 3. Relationship between normalized isoprene emission rates and leaf temperatures observed for sweet gum, eucalyptus, aspen, and velvet beans (symbols) and simulated by eight of the isoprene emission models described in Table 1 (lines).

TABLE 2. Performance Evaluation of Models Described in Table 1

Statistic*		No. of Samples	Results With Isoprene Emission Model†								
			G91	G93	T400	T800	BEIS	L87	HR	EES	ESS
<i>E</i>		16	50	50	66	35	71	34	53	57	44
%Δ <sub>HR</sub>	Total	94	37	36	47	43	46	48	47	46	48
	Range	8–20	21–53	20–53	28–74	25–68	34–72	29–75	36–62	32–73	34–74
<i>r</i> <sup>2</sup>	Total	94	0.86	0.89	0.81	0.79	0.78	0.79	0.33	0.61	0.77
<i>M</i>	Total	94	0.14	0.11	0.24	0.23	0.66	0.24	0.50	0.66	0.25
σ <sub><i>M</i></sub>	Total	94	0.03	0.03	0.04	0.04	0.09	0.04	0.07	0.12	0.04
%Δ <sub>DAY</sub>	Total	6	3.9	3.5	30	20	42	33	33	36	34
	Range	1	0.6–10	0.2–9	9–98	6–52	20–94	12–104	3–52	9–56	11–105

Models were evaluated by using the field measurements described by Guenther et al. (submitted manuscript, 1993).

\* $r^2$ , correlation coefficient; % $\Delta_{DAY}$ , mean percent difference in daily emission rates. The *M* score (defined by equation (4)) and standard deviation of the *M* score ( $\sigma_M$ ) were determined by using bootstrap methods [Efron, 1982].

†Observed emissions were normalized by rates estimated for 30°C and 1000  $\mu\text{mol m}^{-2} \text{s}^{-1}$  by each model. The mean normalized emission rates estimated for the same red oak leaf, *E* (in micrograms of C per gram per hour), are shown as an example.

differences in the daily emission rates predicted by models G91 and G93 were within 0.2 to 10% of observed daily total emission rates. Mean percent differences in observed and predicted daily rates were 3.5% for model G93 and 3.9% for model G91. Mean percent differences between observed and predicted daily rates ranged from 20 to 42% for the other seven models.

The normalized mean square error (*M*) listed in Table 2 provides an overall score of model performance.

$$M = \frac{(E_o - E_p)^2}{\bar{E}_o \bar{E}_p} \quad (4)$$

where  $E_p$  is the emission rate predicted by the model,  $\bar{E}_p$  is the mean predicted emission rate,  $E_o$  is the observed emission rate, and  $\bar{E}_o$  is the mean observed emission rate. The *M* score is a function of three statistical scores (*t*, *F*, and *r*). The *t* is a measure of the bias of magnitude, *F* is a measure of the bias of variance, and the correlation coefficient (*r*) is a measure of the intensity of association. A lower *M* score indicates better overall model performance. Based on the *M* scores and standard deviations, the nine models can be grouped into three categories with significantly different model performances. The standard deviations were estimated with 500 bootstrap iterations by using the methods described by Efron [1982]. Models G91 and G93 displayed the best performance (*M* = 0.11 to 0.14) and were followed

by models T400, T800, L87, and ESS (*M* = 0.23 to 0.26) and models BEIS, HR, and EES (*M* = 0.50 to 0.66).

Figure 4 shows the ability of model G93 to simulate short-term variations in isoprene emission rates from red oak, willow oak, and sweet gum leaves under field conditions. Isoprene emission rates varied over more than 2 orders of magnitude in each case (<0.5 to >50  $\mu\text{g of C g}^{-1} \text{h}^{-1}$ ). The predicted daily total isoprene emissions, i.e., integrated over the entire day, are all within 2% of observed values. Emissions vary by as much as a factor of 5 within a 1-hour period, suggesting that a biogenic emission model should have a time step equal to or less than 1 hour. Over half the predicted emission rates shown in Figure 4 are within 20% of the observed values, and 90% are within a factor of 2.

#### 2.4. Model Sensitivity Analysis

In this section, we consider the sensitivity of model G93 to the coefficients  $\alpha$  (equation (2)) and  $T_M$  (equation (3)). The purpose of this analysis is to determine the magnitudes of the emission rate uncertainties associated with the potential range of values which could be assigned to these two coefficients. The upper portion of Table 3 contains results predicted for a maximum temperature of 35°C and a maximum PAR of 1500  $\mu\text{mol m}^{-2} \text{s}^{-1}$ . The bottom part of Table 3 illustrates that the results of this analysis are sensitive to both daily maximum temperature and light intensity.

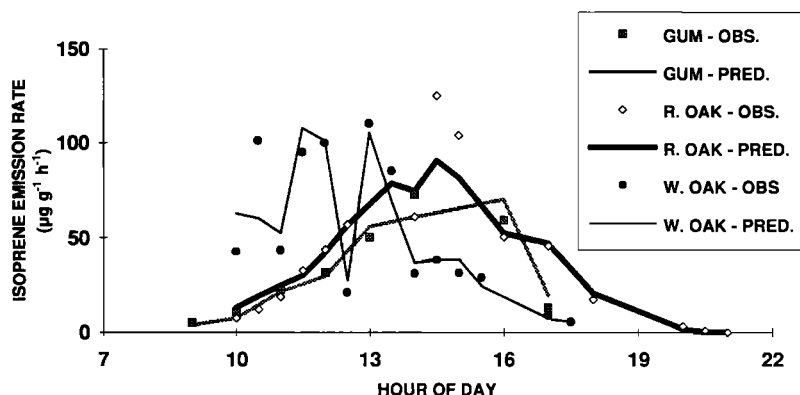


Fig. 4. Diurnal isoprene emission rate variation observed (symbols) at the ROSE field site (A. Guenther et al., submitted manuscript, 1993) and simulated (lines) by model G93 (described in Table 1).

TABLE 3. Sensitivity Analysis of Isoprene Emission Model G93 (Equations (1)–(3))

$\alpha$	$T_M$	$T_{max}$	$L_{max}$ ( $\mu\text{mol m}^{-2}$ $\text{s}^{-1}$ )	Total Percent Difference*		
				Daily	Morning	Midday
0.0007	314	35	1500	-16	-36	-5.9
0.0017	314	35	1500	-5.9	-15	-1.8
0.0037	314	35	1500	3.5	10	0.8
0.0047	314	35	1500	5.7	16	1.2
0.0057	314	35	1500	7.1	21	1.5
0.0027	310	35	1500	-14	-0.9	-8.8
0.0027	312	35	1500	-5.5	-0.3	-3.4
0.0027	316	35	1500	3.5	0.2	2.1
0.0027	318	35	1500	5.5	0.3	3.2
0.0017	314	35	2000	4.9	6.1	0.4
0.0017	314	35	1500	6.9	9.7	1.5
0.0017	314	35	1000	11	16	4.3
0.0017	314	35	500	25	34	16
0.0017	314	35	300	40	49	32
0.0027	318	20	1500	0.1	0.1	0.1
0.0027	318	30	1500	1.3	0.1	0.7
0.0027	318	40	1500	20	1.3	13
0.0027	318	45	1500	51	5.8	37

\*Percent differences in emissions were estimated for a 24-hour period (daily total), a 3-hour period between 0600 and 0900 UT (morning total), and a 6-hour period between 0900 and 1500 UT (midday total).

We generated sets of 24 hourly average temperatures by using a sine function to vary between the assigned daily minimum ( $T_{min}$ ) and daily maximum temperatures ( $T_{max}$ ). Hourly average PAR fluxes were generated similarly except that PAR was set equal to zero before 0600 and after 1800 UT. We used model G93 to estimate variations in hourly average emission rates for two sets of 24-hour periods. Emission rates in the first set were calculated by using model G93 with  $\alpha = 0.0027$  and  $T_M = 314$ . Emissions for the second set were calculated with a range of values for  $\alpha$  (0.0007–0.0057) and  $T_M$  (310–318), which is similar to the range observed in laboratory experiments. In each case we calculated the percent difference in the daily (24 hour) total, morning (0600–900 UT) total, and midday (0900–1500 UT) total emission rates. Results of this analysis are in the top section of Table 3. If the assumed value of  $\alpha$  is less than the actual value, the model will underestimate emissions when  $L < 1000 \mu\text{mol m}^{-2} \text{s}^{-1}$  and overestimate when  $L > 1000 \mu\text{mol m}^{-2} \text{s}^{-1}$ . If the assumed value of  $T_M$  is less than the actual value, the model will underestimate emissions at high (>33°C) temperatures.

The PAR and temperature regimen used for the following analysis ( $T_{min} = 20^\circ\text{C}$ ;  $T_{max} = 35^\circ\text{C}$ ;  $L_{max} = 1500 \mu\text{mol m}^{-2} \text{s}^{-1}$ ) represents a hot summer day at temperate latitudes, which provides the potential for very high isoprene fluxes. Estimates of  $\alpha$  between 0.0017 and 0.0047 result in differences in daily, morning, and midday fluxes of less than or equal to 6, 16, and 2%, respectively. The highest (0.0057) and lowest (0.0007) values of  $\alpha$  observed in the laboratory experiments described above result in percent differences in daily, morning, and midday fluxes of 7–16, 21–36, and 1.5–5.9%, respectively. The percent differences resulting from perturbation of  $T_M$  over the range observed in laboratory experiments (310–318) were as high as 14% of the daily total, 1% of the morning total, and 8.8% of the midday total emission rates.

To assess the sensitivity of these results to variations in the daily temperature regimen, we set  $\alpha = 0.0017$  and  $T_M = 318$  and examined the effect of varying either the maximum temperature or the maximum light intensity. The results suggest that the error associated with uncertainties in  $\alpha$  is sensitive to the daily maximum light intensity and the error associated with uncertainties in  $T_M$  is sensitive to the daily maximum temperature. Increasing  $T_{max}$  from 20 to 40°C results in large increases (0.1–20%) in the difference between estimated fluxes. A decrease in the maximum PAR from 2000 to 300  $\mu\text{mol m}^{-2} \text{s}^{-1}$  results in significant increases in the uncertainties associated with estimated emission rate variations.

### 3. MONOTERPENE EMISSIONS

#### 3.1. Monoterpene Model Description and Evaluations

Short-term variations in monoterpene emissions have been attributed to changes in leaf temperature [Dement *et al.*, 1975; Tingey, 1981; Juuti *et al.*, 1990; Guenther *et al.*, 1991], relative humidity [Dement *et al.*, 1975], foliar moisture [Lamb *et al.*, 1985], and light intensity [Steinbrecher *et al.*, 1988]. The role of relative humidity, foliar moisture, and light intensity in controlling short-term variations is not clear, and there are currently no quantitative descriptions of the relationship between monoterpene emission rates and these environmental variables. Changes in relative humidity and light intensity appear to have a negligible impact on short-term variations in monoterpene emissions for at least some plants [e.g., Tingey, 1981; Juuti *et al.*, 1990; Guenther *et al.*, 1991]. Biogenic emission models typically use equation 5 to simulate the temperature dependence of monoterpene emission rates [e.g., Pierce and Waldruff, 1991; Roselle *et al.*, 1991; Lamb *et al.*, 1987].

$$M = M_s \cdot \exp(\beta(T - T_s)) \quad (5)$$

where  $M$  is monoterpene emission rate at temperature  $T$  (K),  $M_s$  is monoterpene emission rate at a standard temperature  $T_s$  (K), and  $\beta$  ( $\text{K}^{-1}$ ) is an empirical coefficient. Equation (5) can account for diurnal variations in monoterpene emissions but may not fully account for seasonal variations [Yokouchi and Ambe, 1984].

The coefficient  $M_s$ , the emission rate at a standard temperature, scales emissions to account for emission rate variation not specifically resulting from temperature. This may include differences due to genotype, nutrient availability, phenology, relative humidity, foliar moisture, or stresses. The value of  $M_s$  can vary over more than 3 orders of magnitude among different plant species and monoterpenes.

The coefficient  $\beta$  establishes the temperature dependence of emission rate in equation (5). The estimates of  $\beta$  listed in Table 4 vary from 0.057 to 0.144  $\text{K}^{-1}$ , but about half the estimates fall within the range of  $0.09 \pm 0.015 \text{ K}^{-1}$ , and 75% of the 28 estimates fall within the range of  $0.09 \pm 0.025 \text{ K}^{-1}$ . The differences in the reported estimates of  $\beta$  can be attributed to (1) leaf-to-leaf and seasonal emission rate variations, (2) different vapor pressures and solubilities for different monoterpenes, (3) different storage and emission pathways in different plants, particularly between conifers and nonconiferous plants, and (4) experimental error.

Different experimental protocols were used to collect the

TABLE 4. Estimates of Coefficient  $\beta$  ( $K^{-1}$ ), Which Defines Temperature Dependence of Monoterpene Emission Rates in (5)

Vegetation Species	Monoterpene	$\beta$	Reference
<i>Abies concolor</i>	$\alpha$ -pinene	0.144	Rasmussen [1972]
<i>Pinus strobus</i>	$\alpha$ -pinene	0.110	Rasmussen [1972]
<i>Pinus taeda</i>	$\alpha$ -pinene	0.139	Rasmussen [1972]
<i>Pinus ponderosa</i>	$\alpha$ -pinene	0.099	Rasmussen [1972]
<i>Salvia mellifera</i>	camphor	0.068*	Dement et al. [1975]
<i>Salvia mellifera</i>	camphor	0.120†	Dement et al. [1975]
<i>Pinus elliotii</i>	$\alpha$ -pinene	0.091	Arnts et al. [1978]
<i>Pinus elliotii</i>	$\alpha$ -pinene	0.067	Tingey [1981]
<i>Pinus elliotii</i>	$\beta$ -pinene	0.077	Tingey [1981]
<i>Pinus elliotii</i>	myrcene	0.076	Tingey [1981]
<i>Pinus elliotii</i>	limonene	0.074	Tingey [1981]
<i>Pinus elliotii</i>	$\beta$ -phellandrene	0.065	Tingey [1981]
<i>Pinus densiflora</i>	$\alpha$ -pinene	0.108	Yokouchi and Ambe [1984]
<i>Picea sitchensis</i>	$\beta$ -pinene	0.085	Evans et al. [1985]
<i>Picea sitchensis</i>	$\alpha$ -pinene	0.100	Evans et al. [1985]
<i>Picea sitchensis</i>	myrcene	0.062	Evans et al. [1985]
<i>Picea sitchensis</i>	camphene	0.067	Evans et al. [1985]
<i>Picea engelmannii</i>	$\alpha$ -pinene	0.114	Evans et al. [1985]
<i>Picea engelmannii</i>	$\beta$ -pinene	0.112	Evans et al. [1985]
<i>Picea engelmannii</i>	$\beta$ -phellandrene	0.079	Evans et al. [1985]
<i>Picea engelmannii</i>	camphene	0.077	Evans et al. [1985]
<i>Picea engelmannii</i>	myrcene	0.057	Evans et al. [1985]
Various	$\alpha$ -pinene	0.131	Lamb et al. [1987]
<i>Pinus radiata</i>	$\alpha$ -pinene	0.085	Juuti et al. [1990]
<i>Eucalyptus globulus</i>	$\alpha$ -pinene	0.094	Guenther et al. [1991]
<i>Eucalyptus globulus</i>	1,8-cineole	0.100	Guenther et al. [1991]
<i>Pinus taeda</i>	$\alpha$ -pinene	0.089	A. Guenther et al. (submitted manuscript 1993)
<i>Pinus taeda</i>	$\beta$ -pinene	0.092	A. Guenther et al. (submitted manuscript 1993)

\*Branch kept at a temperature of 10°C before measurement.

†Branch kept at a temperature of 40°C before measurement.

data from which the estimates of  $\beta$  in Table 4 were calculated, making direct comparisons between published values problematic, and in several cases, data were collected from different plant species or at different seasons. If seasonal and spatial variations in emissions are neglected, then pooling of data from leaves with different values of  $M_s$  will lead to biased estimates of  $\beta$ . For example, the temperature dependence reported by Lamb et al. [1987] (equivalent to  $\beta = 0.131$  when converted to  $\log_{10}$ ) may be biased by higher values of  $M_s$  for the plants species measured at southern U.S. sites (primarily at temperatures between 22 and 38°C) compared with the values of  $M_s$  for plants at northern U.S. sites (primarily at temperatures between 8 and 20°C). Juuti et al. [1990] avoided this problem by measuring emissions rates from a single plant. Guenther et al. (1991, submitted manuscript, 1993) pooled data from different plants but first normalized the data by dividing each emission rate measurement by the estimate of  $M_s$  determined for each plant on each day. In each of these studies the estimated values of  $\beta$  are close to 0.09.

Detailed monoterpene emission rate models which base monoterpene emission rates on environmental conditions, leaf morphology, and needle resin content have been proposed [e.g., Tingey et al., 1991]. These detailed models cannot be evaluated with existing field measurement data sets and require input variables which are not currently available on regional scales. The model developed by Tingey et al. [1991] predicts that the temperature dependence of monoterpene emissions will vary with vegetation species and the monoterpene being emitted.

Estimates of  $\beta$  range from 0.067 to 0.14 for a single monoterpene,  $\alpha$ -pinene, from 10 plant species listed in Table 4. Estimates of  $\beta$  for five different monoterpenes range from 0.067 to 0.0769 for *Pinus elliotii* [Tingey, 1981] and 0.057 to 0.114 for *Picea engelmannii* [Evans et al., 1985]. There are also differences in the estimates of  $\beta$  for a single monoterpene,  $\alpha$ -pinene, from the same plant species: 0.089 and 0.139 for *Pinus taeda* and 0.067 and 0.091 for *Pinus elliotii*. Dement et al. [1975] report that  $\beta$  is also dependent on the temperature of the plant before measurement. The estimates of  $\beta$  shown in Table 4 do not indicate a clear relationship between  $\beta$  and monoterpene or vegetation species. A systematic investigation is required to understand the observed variability in  $\beta$ .

### 3.2. Model Sensitivity Analysis

In this section, we consider the sensitivity of equation (5) to the coefficient  $\beta$ . This analysis relates uncertainty in the value of  $\beta$  to the resulting uncertainties in estimated monoterpene emission rates. The upper portion of Table 5 contains results for a day with a minimum temperature of 22°C and maximum temperature of 37°C. The bottom part of Table 5 shows how the results of this analysis are sensitive to daily minimum and maximum temperatures. The hourly average temperatures used for this analysis were generated by using the procedures described above in section 2.2.

We simulated two sets of hourly average emission rates for 24-hour periods by using equation (5) with  $T_s = 303.15$  K. In the first set,  $\beta$  was equal to our best estimate of 0.09.

TABLE 5. Percent Differences Between Monoterpene Emission Rates Estimated by Using Equation (5) With  $\beta = 0.09 \text{ K}^{-1}$  and With Alternative Values of  $\beta$  Ranging From 0.057 to 0.144

$\beta$	Temperature, °C		Percent Difference†			
	$T_{\min}$	$T_{\max}$	Daily Total	Daytime Total	Hour of $T_{\min}$	Hour of $T_{\max}$
0.057	22	37	-2.8	-7.8	30	-21
0.065	22	37	-2.3	-6.1	22	-19
0.075	22	37	-1.5	-3.9	13	-10
0.09	22	37	0.0	0.0	0	0
0.105	22	37	2.0	4.4	-11	11
0.115	22	37	3.5	7.7	-18	19
0.144	22	37	9.1	19	-35	46
0.065	30	30	0.0	0.0	0	0
0.065	25	35	-1.6	-4.1	13	-11
0.065	23	38	-4.7	-8.4	19	-18
0.065	20	40	-6.1	-11	28	-22
0.065	20	40	-6.1	-11	28	-22
0.065	15	35	6.4	0.9	45	-12
0.065	10	30	21	14	65	0
0.065	0	20	55	47	112	28

\*Standard temperature ( $T_s$ ) = 30°C.

†Percent differences in emission rates are estimated for a 24-hour period (daily total), a 12-hour period between 0600 and 1800 UT (daytime total), hour 0600 (hour of  $T_{\min}$ ), and hour 1400 (hour of  $T_{\max}$ ).

The range of values shown in Table 4 (0.057–0.144) was used to represent  $\beta$  in the second set of emission rates. The percent differences between emissions calculated with the different values of  $\beta$  were calculated for each 24-hour period (daily total), for a 12-hour period between 0600 and 1800 UT, for hour 0600 (hour of  $T_{\min}$ ), and for hour 1800 (hour of  $T_{\max}$ ).

The upper portion of Table 5 shows that if we use equation (5) with  $\beta = 0.09$ , we can expect percent differences in hourly emission rates to be less than 25% if the actual value of  $\beta$  is between 0.065 and 0.115. The percent difference in estimated total daily (24 hour) and total daytime (12 hour) variations are considerably less than 10%. The lower percent differences in total emissions occur because if the model overestimates emissions when  $T < T_s$ , i.e., the assumed value of  $\beta$  is less than the actual value, then the model underestimates emissions when  $T > T_s$ .

To assess the sensitivity of these results to the daily temperature regimen, we set  $\beta = 0.065$  and examined the effect of varying either the temperature range (middle section of Table 5) or the daily average temperature (bottom of Table 5). These results show that the error associated with uncertainties in  $\beta$  is sensitive to both the mean daily temperature and the range of temperatures encountered. An increase in the difference between the daily average temperature and the temperature to which emissions rates have been normalized,  $T_s$ , can significantly increase errors in fluxes estimated with equation (5). The errors in daily and daytime variations in emissions increase from around 10% or less if the daily average temperature is within 5°C of  $T_s$  to around 50% if  $T_s$  is 20°C greater than the daily average temperature.

#### 4. SUMMARY AND RECOMMENDATIONS

The chemical time steps used in regional tropospheric photochemical models vary depending on chemical reaction

rates but typically range from 10 to 60 seconds [e.g., *Roselle et al.*, 1991]. Accurate simulation of diurnal biogenic hydrocarbon emission rate variations is required to provide realistic hydrocarbon concentrations at each chemical time step. Leaf temperature plays the major role in determining diurnal monoterpene emission rate variations, while diurnal isoprene emission rate variations are determined by both leaf temperature and light intensity. Light and temperature also play an important role in controlling seasonal, year-to-year, and spatial variations.

The temperature dependence of isoprene emission appears to be associated with isoprene synthase enzyme activity [*Monson et al.*, 1992]. Isoprene emissions respond to light with a linear increase up to a light saturation point. We recommend using model G93, described in Table 1, to simulate isoprene emission rate variations associated with light and temperature. This model performs well for a variety of plant species and performs significantly better than other models which have been used to simulate isoprene emission rate variation. The improved performance of this model is probably a result of its partial basis in the biochemical mechanisms that control isoprene emissions. It should be noted that the computational expense and data input requirements of model G93 are not prohibitive and that the model can be easily incorporated into regional and global biogenic hydrocarbon emission models. While this model provides a good first-order approximation, there may be additional factors which influence short-term variations in isoprene emission rates. These factors include but are not limited to growth environment, species-to-species variations among plants, maximum emission rates, leaf age, and season.

The temperature dependence of monoterpene emission rates is related to monoterpene vapor pressure and increases exponentially with increasing temperature. Monoterpene emission rate behavior varies among monoterpenes, vegetation species, and other factors, but a simple exponential relationship between temperature and emission provides a good first-order approximation. On the basis of existing data, we recommend that equation (5) be used with a value of  $\beta = 0.09 \text{ K}^{-1}$ .

Short-term (hours to days) monoterpene and isoprene emission rate variation can be simulated by using the models described above. The uncertainties vary depending on environmental conditions but are typically <25% for individual hours and <10% for daily totals estimated for the hot sunny days associated with high biogenic hydrocarbon fluxes at temperate latitudes. More accurate descriptions of biogenic emission rate variations may be obtained by incorporating second-order effects into these general models. This can occur only if model improvements are accompanied by a means of estimating the variables needed to initialize and drive additional model components.

**Acknowledgments.** This research was partially supported by the U.S. Environmental Protection Agency, Research Triangle Park, N. C., under Interagency Agreement Grant DW49934973-01-0, and by U.S. EPA grant R-815995-01-0 and NSF grant ATM-9007849. The National Center for Atmospheric Research is sponsored by the National Science Foundation. We thank Brett Taylor for assistance in laboratory isoprene measurements.

#### REFERENCES

Arnts, R., R. Seila, R. Kuntz, F. Mowry, K. Knoerr, and A. Dudgeon, Measurement of  $\alpha$ -pinene fluxes from a Loblolly Pine



- forest, *Conf. Proc. 4th Joint Conf. Sensing Environ. Pollutants*, pp. 829–833, 1978.
- Chameides, W., R. Lindsay, J. Richardson, and C. Kiang, The role of biogenic hydrocarbons in urban photochemical smog: Atlanta as a case study, *Science*, **241**, 1473–1475, 1988.
- Chameides, W., et al., Ozone precursor relationships in the ambient atmosphere, *J. Geophys. Res.*, **97**, 6037–6055, 1992.
- Dement, W., B. Tyson, and H. Money, Mechanism of monoterpene volatilization in *Salvia mellifera*, *Phytochemistry*, **14**, 2555–2557, 1975.
- Efron, B., The jackknife, the bootstrap and other resampling plans, *CBMS-NSF-38*, Soc. Ind. Appl. Math., Philadelphia, Pa., 1982.
- Evans, R., D. Tingey, and M. Gumpertz, Interspecies variation in terpenoid emissions from Engelmann and Sitka spruce seedlings, *For. Sci.*, **31**, 132–142, 1985.
- Fall, R., and R. Monson, Isoprene emission rate and intercellular isoprene concentration as influenced by stomatal distribution and conductance, *Plant Physiol.*, **100**, 987–982, 1992.
- Guenther, A., R. Monson, and R. Fall, Isoprene and monoterpene emission rate variability: Observations with eucalyptus and emission rate algorithm development, *J. Geophys. Res.*, **96**, 10,799–10,808, 1991.
- Harley, P., and J. Tenhunen, Modeling the photosynthetic response of C3 leaves to environmental factors, in *Modeling Crop Photosynthesis—from Biochemistry to Canopy*, *Crop Soc. Am. Spec. Publ.*, **19**, Madison, Wisc., 1991.
- Hills, A., and P. Zimmerman, Isoprene measurement by ozone-induced chemiluminescence, *Anal. Chem.*, **62**, 1055–1060, 1990.
- Johnson, F., H. Eyring, and R. Williams, The nature of enzyme inhibitions in bacterial luminescence: Sulfanilamide, urethane, temperature, pressure, *J. Cell Comp. Physiol.*, **20**, 247–268, 1942.
- Juuti, S., J. Arey, and R. Atkinson, Monoterpene emission rate measurements from a Monterey Pine, *J. Geophys. Res.*, **95**, 7515–7519, 1990.
- Kuzma, J., and R. Fall, Leaf isoprene emission rate is dependent on leaf development and the level of isoprene synthase, *Plant Physiol.*, in press, 1993.
- Lamb, B., H. Westberg, and G. Allwine, Biogenic hydrocarbon emissions from deciduous and coniferous trees in the United States, *J. Geophys. Res.*, **90**, 2380–2390, 1985.
- Lamb, B., A. Guenther, D. Gay, and H. Westberg, A national inventory of biogenic hydrocarbon emissions, *Atmos. Environ.*, **21**, 1695–1705, 1987.
- Liu, S. C., M. Trainer, F. Fehsenfeld, D. D. Parrish, E. J. Williams, D. W. Fahey, G. Hübner, and P. C. Murphy, Ozone production in the rural troposphere and the implications for regional and global ozone distributions, *J. Geophys. Res.*, **92**, 4191–4207, 1987.
- Monson, R., A. Hills, P. Zimmerman, and R. Fall, Studies of the relationship between isoprene emission rate and CO<sub>2</sub> or photon-flux density using a real-time isoprene analyzer, *Plant Cell Environ.*, **14**, 517–523, 1991.
- Monson, R., C. Jaeger, W. Adams, E. Driggers, G. Silver, and R. Fall, Relationships among isoprene emission rate, photosynthesis, and isoprene synthase activity as influenced by temperature, *Plant Physiol.*, **92**, 1175–1180, 1992.
- Pierce, T., and P. Waldruff, PC-BEIS: A personal computer version of the biogenic emissions inventory system, *J. Air Waste Manage. Assoc.*, **41**, 937–941, 1991.
- Rasmussen, R., What do the hydrocarbons from trees contribute to air pollution?, *JAPCA*, **22**, 537–543, 1972.
- Roselle, S., T. Pierce, and K. Schere, The sensitivity of regional ozone modeling to biogenic hydrocarbons, *J. Geophys. Res.*, **96**, 7371–7394, 1991.
- Sharpe, P., and D. De Michelle, Reaction kinetics of poikilothermic development, *J. Theor. Biol.*, **64**, 649–670, 1977.
- Smith, E., The influence of light and carbon dioxide on photosynthesis, *Gen. Physiol.*, **20**, 807–830, 1937.
- Steinbrecher, R., R. Schonwitz, and H. Ziegler, Emission of monoterpenes from needles of *Picea abies* (L.) Karst under field conditions, *19th Int. Symp. Essential Oils Other Nat. Substrates*, Landenberghaus Greifensee, 1988.
- Tingey, D., The effect of environmental factors on the emission of biogenic hydrocarbons from live oak and slash pine, in *Atmospheric Biogenic Hydrocarbons*, edited by J. Bufalini and R. Arnts, pp. 53–72, Butterworth, Stoneham, Mass., 1981.
- Tingey, D., D. Turner, and J. Weber, Factors controlling the emissions of monoterpenes and other volatile organic compounds, in *Trace Gas Emissions by Plants*, edited by T. Sharkey, H. Mooney, and E. Holland, pp. 93–119, Academic, San Diego, Calif., 1991.
- Yokouchi, Y., and Y. Ambe, Factors affecting the emission of monoterpenes from Red Pine (*Pinus densiflora*), *Plant Physiol.*, **75**, 1009–1012, 1984.
- A. B. Guenther, P. R. Zimmerman, and P. C. Harley, Atmospheric Chemistry Division, National Center for Atmospheric Research, P. O. Box 3000, Boulder, CO 80307-3000.
- R. K. Monson, Department of EPO Biology, University of Colorado, Boulder, CO 80309.
- R. Fall, Department of Chemistry and Biochemistry and Cooperative Institute for Research in Environmental Sciences, University of Colorado, Boulder, CO 80309.

(Received October 16, 1992;  
revised February 24, 1993;  
accepted February 26, 1993.)